The RF Front-end of a Blood Flow Sensor for Vascular Graft Applications

Kai Kang, Pradeep Basappa Khannur, Rui-Feng Xue, Woo Tae Park, Kotlanka Ramakrishna, Yuanjin Zheng and Minkyu Je
Institute of Microelectronics, A*STAR (Agency for Science, Technology and Research), Singapore
E-mail: kangkai@ieee.org

***Abstract*— This paper presents an RF front-end of a fully integrated inductively powered implantable circuits for blood flow measurement, which are embedded within vascular prosthetic grafts for early detection of graft degradation or failure. The effect of human body on the helix coil design has been carefully characterized. An equivalent circuit model of the coil has been developed. An adaptive link compensation technique was adopted in the backscattering modulator design. A highly efficient rectifier was designed to achieve 65% efficiency.**

I. INTRODUCTION

Hundreds of vascular prosthetic grafts are implanted everyday for haemodialysis or bypass purposes all over the world. Prosthetic grafts are frequently used in vascular surgery in the context of bypass surgery for lower limb ischemia or as a conduit for haemodialysis in renal failure. In these settings, graft failure can result in deleterious outcomes for the patients i.e. worsening ischemia, inability to undergo haemodialysis. Insufficient blood flow rates in these grafts are predictive of subsequent graft thrombosis and failure. Underlying this is the presence of stenoses in the graft or downstream from the graft. Variations in flow rates can localize the position of significant stenosis that may result in graft thrombosis. Flow rate monitoring provides an indication for early intervention to prevent graft failure.

As such, a large amount of resources are devoted to detecting failing grafts vis-a-vis decreasing flow rates. An implantable system that can provide convenient monitoring of blood flow in vascular prosthetic grafts with a simple hand-held device is desired. With the sensor-embedded graft, the failing graft can be detected at its earlier stage thus implementing early intervention strategies.

The RF front end of the proposed implantable blood flow sensor includes a helix coil and four other circuit blocks parallel connecting to the coil, as shown in Fig.1. These four circuits are a modulator, a rectifier, a clock extractor and an ASK demodulator. In this paper, we only focus on designing of the helix coil, the rectifier and the backscattering modulator.

II. BUILDING BLOCKS

Passive RFID technique has been widely applied in bio-implantable sensors. Using this technique, power can be delivered to the tag through an inductive coupling link. This is the most attracting feature to the bio-implantable sensors because battery is not necessary. Cost and size of the sensors can be therefore reduced. As there is no battery to power the ASIC, it is utmost important how efficiently the RF energy is coupled from the external device. Hence, the helix coil and rectifier are designed to achieve a high efficiency.

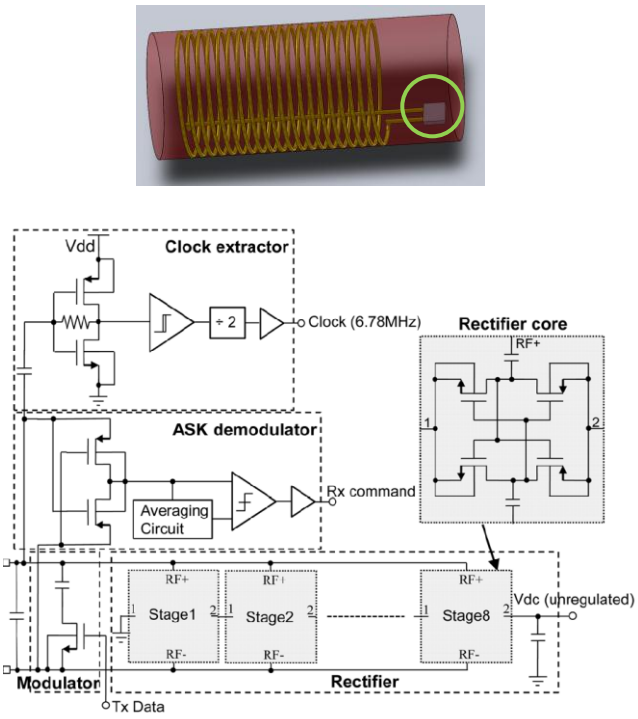

Fig. 1 The diagram of the RF front-end of an implantable blood flow sensor.

A. Helix Coil

As shown in the Fig. 1, the helix coil is used to obtain the energy from outside of the human body through magnetic coupling between itself and the reader's coil. In the meantime, it also functions as an antenna of the sensor to receive and transmit data.

The helix is fabricated using titanium, a bio-compatible material. Its helix radius is 3 mm. The polygon radius, pitch and turns are 0.15 mm, 0.3 mm and 20 respectively.

Proceedings of the Second APSIPA Annual Summit and Conference, pages 741–744,
Biopolis, Singapore, 14-17 December 2010.

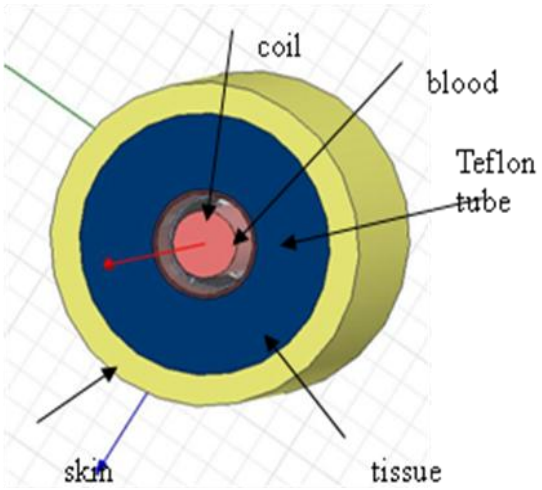

Fig. 2. The helix coil is embedded in a multi-layer cylinder to mimic the human body environment.

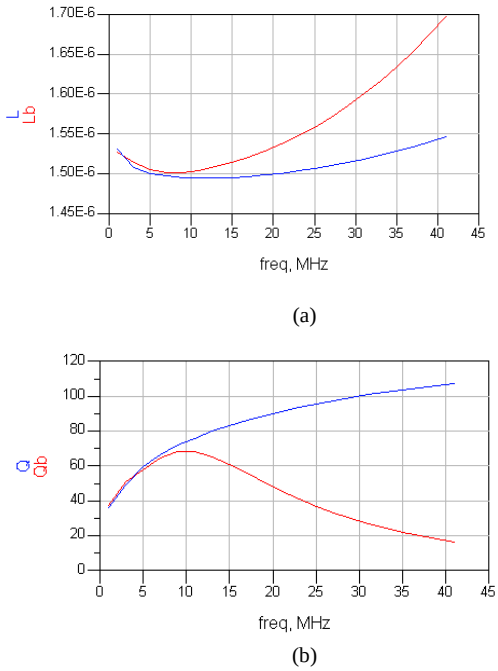

Fig. 3. The effective (a) inductance and (b) quality factor of the coil with (red color) and without (blue color) considering human body environments.

In order to investigate the effects of human bodies on the coil, the helix coil is embedded in a multilayer cylinder, as shown in the Fig. 2. This cylinder is used to mimic the blood, tissue and skin. The simulation was run in the HFSS, a full-wave EM software. The simulated effective inductance and quality factor of the coil in and out of body are plotted in the Fig. 3. It is obvious that human body will introduce loss and therefore degrade the performance of the coil. As shown in the Fig. 3, the peak of Q is reduced considerably. The parasitic capacitance also lowers the self-resonant frequency of the coil and then operation frequency as a result. The peaking of the inductance is caused by the resonance of the coil at lower frequency compared to the one without including human body.

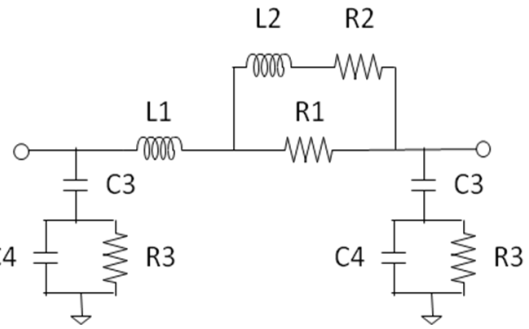

Fig. 4. The equivalent circuit model of the coil.

In order to design coil together with other circuits, an equivalent circuit model of the coil is highly desired, which can be simulated in SPICE-liked circuit simulators. Fig. 4 shows a model. The inductance L_1 and resistance R_1 represent the DC impedance of the coil. The laddered series branch including inductance L_2 and resistance R_2 accounts loss at high frequencies due to skin and proximity effects. Due to symmetry of the coil, the two shunt branches are identical, each of which consists of a capacitor series connecting to a parallel RC tank. The modeled results are compared with the results using HFSS in terms of inductance and Q, and plotted in Fig. 5. They agree each other well.

B. Modulator with Adaptive Link Compensation

Variations in the thickness of tissue, bone and skin are expected to different people. These variations will affect the resonance frequency of the tank shared by both the rectifier and modulator. To compensate this frequency shift, the tank resonance frequency has to be programmable to either higher or lower frequencies.

The principle of the backscattering modulation is illustrated in Fig. 6. The variation in tank impedance will change the tank voltage because impedance variation will change the self resonance frequency of the tank. There are basically two methods to change the tank impedance. One is the capacitive tuning, the other one is the resistive tuning, which are shown in the Fig. 7.

In the capacitive backscattering modulator, the M_1 is controlled by the baseband data. Therefore, the capacitor C_1 is used to change the tank impedance, which in turn changes the voltage. As a result, backscattering modulated signal is generated [1-2].

Similar to the capacitive backscattering modulator, M_1 is controlled by the baseband in a resistive backscattering modulator. R_1 will be included into the tank impedance by turn on/off the M_1. As a result, the tank impedance and voltage can be varied between two values. Then, the modulated backscattering signal is generated [1].

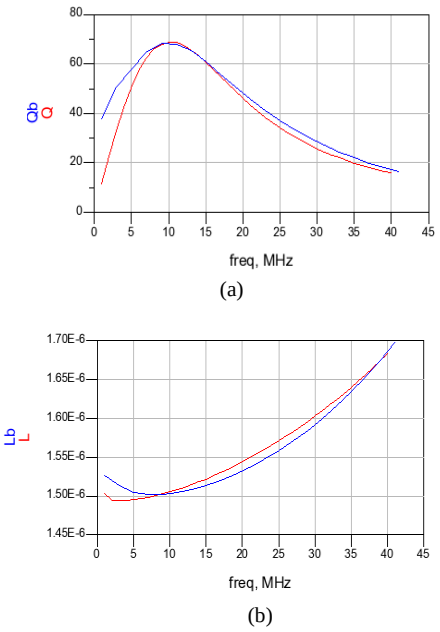

Fig. 5. The modeled (red) and EM simulated (blue) effective (a) inductance and (b) quality factor of the coil.

In the both prior arts, the tank impedance can only be increased so that the self-resonance frequency can only be decreased. However, if the default tank capacitance is C_H due to variations from fabrication and human body, as shown in Fig. 6, the tank impedance needs to be reduced to achieve the maximum modulation depth. Previous techniques cannot provide such solution. Therefore, we propose a new adaptive link compensation technique which can both increase and decrease the tank impedance, as shown in Fig. 8.

This adaptive link compensation has following advantages

- Tank capacitance C_{tank} can be either increased or decreased
- Tank resonance frequency can be either reduced or increased
- Backscattering Modulator and tank tuning share the same tank circuits
- Modulation depth control is achieved

M0 and M1 are implemented using PMOS, and their default status is on. M2 and M3 are implemented using NMOS, and their default state is off. A logic block is introduced to select certain combination of the capacitors to achieve maximum modulation depth. The capacitors' values can be determined by

$$C_{tank} = C_{01} + C_{11} \quad (1)$$

$$C_{02} = \frac{C_{01}^2}{\alpha_1 C_{tank}} - C_{01} \quad (2)$$

$$C_{12} = \frac{C_{11}^2}{\beta_1 C_{tank}} - C_{11} \quad (3)$$

$$C_2 = \alpha_2 C_{tank} \quad (4)$$

$$C_3 = \beta_2 C_{tank} \quad (5)$$

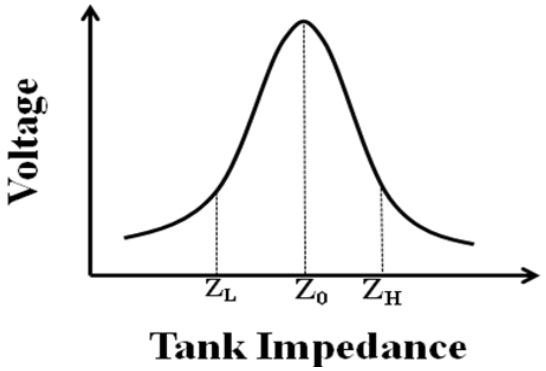

Fig. 6. The diagram illustrates the principle of the backscattering modulation.

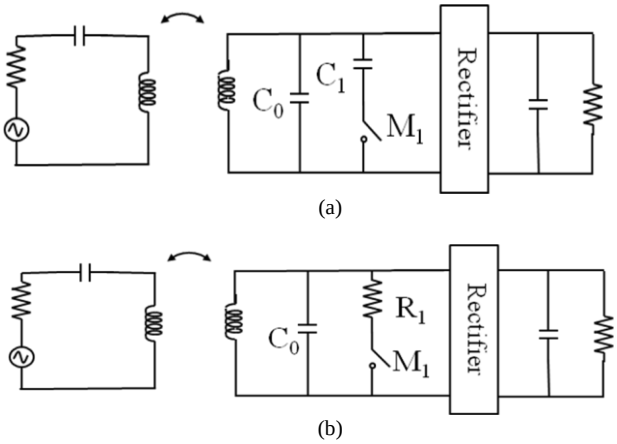

Fig. 7. The schematic of a capacitive backscattering modulator and a resistive backscattering modulator.

Turn on/off the switch M_0-M_3, the tank impedance will be changed by

- M_0 off: C_{tank} reduces α_1
- M_1 off: C_{tank} reduces β_1
- M_2 on: C_{tank} increases α_2
- M_3 on: C_{tank} increases β_2

C. Rectifier

The power conversion efficiency (PCE) of the rectifier is one of the most important parameters. In order to increase PCE of the rectifier, the dropout voltage of the rectifier needs to be minimized. This can be realized by either increasing the W/L ratio of transistors or using Vth cancellation technique. The dynamical Vth cancellation technique was adopted in this design. Minimizing substrate leakage current can also help to increase PCE. In the meanwhile, latch-up needs to be avoided. In this paper, for converting AC energy to DC energy, an eight-stage differential-drive rectifier is used [3]. The schematic of the rectifier is shown in Fig. 1. The rectifier core has a cross-coupled bridge configuration. A differential-drive

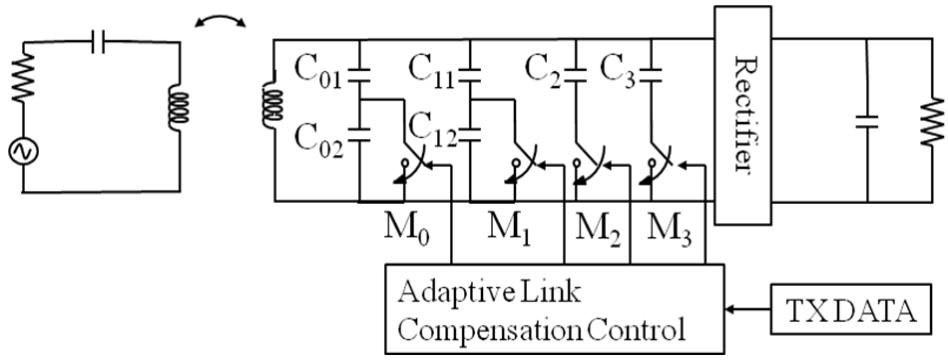

Fig. 8. The proposed backscattering modulator with adaptive link compensation control

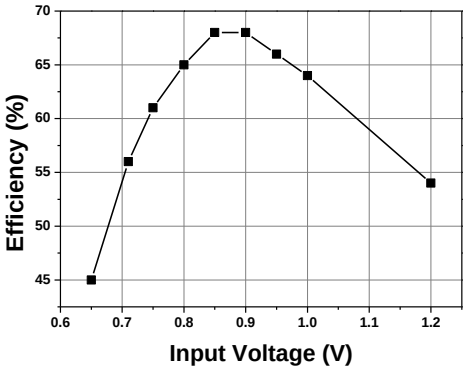

Fig. 9. The simulated efficiency of the rectifier as a function of input voltage.

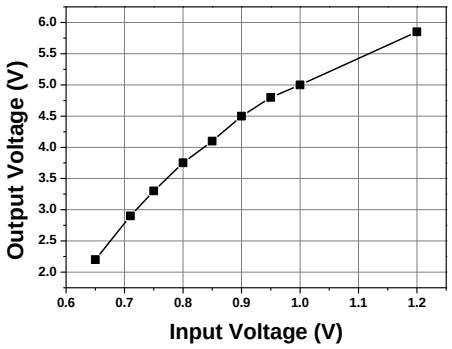

Fig. 10. The simulated output voltage of the rectifier as a function of input voltage.

active gate bias mechanism enables to achieve both low ON-resistance and small reverse leakage of diode-connected MOS transistors at the same time, resulting in a high PCE. Unit stages are serially stacked along the DC path and connected in parallel to the input RF terminals. By using this multi-stage configuration, appropriate DC output voltage is obtained at the optimal operating point where the PCE is maximized. As shown in Fig. 9, the maximum PCE is 65% with a load resistor of 20 kΩ. As expected, the output voltage increases with input voltage, as shown in Fig. 10. The chip photo is

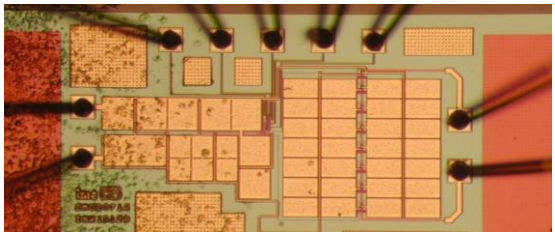

Fig. 11. Chip photo

shown in Fig. 11. The circuits is fabricated by a commercial 0.18 μm CMOS process.

III. CONCLUSIONS

The RF front-end of a blood flow sensor, which is embedded within vascular prosthetic grafts for early detection of graft degradation or failure, has been presented in this paper. The helix coil, the backscattering modulator and the rectifier included in the RF front-end have been discussed in detail. The human body can degrade the quality factor of the helix coil and make the coil design become a challenge. The equivalent circuit model of the coil is developed to allow the coil to be simulated with other circuits in Spectre simulator. The adaptive link compensation technique is developed to compensate variations of tank impedance introduced by fabrication and human body. A highly efficient rectifier is designed and 65% efficiency is achieved.

Acknowledgement: This work was supported in part by A*Star science and research council under Grant 0921480069

REFERENCES

[1] B. C. Yeung and W. G. Yeoh, "Air-interfacing microwave passive RFID tag in bulk CMOS", *IEEE RFIT*, pp. 65-69, 2005

[2] S. O'Driscoll, A. S. Y. Poon and T. H. Meng, "A mm-sized implantable power receiver with adpative link compensation", *ISSCC* 2009.

[3] Koji Kotani, Atushi Sasaki and Takashi Ito, "High-efficiency differential-drive CMOS rectifier for UHF RFIDs," *IEEE Journal of Solid-State Circuits*, vol. 44, no. 11, pp. 3011-3018, November 2009.